

An Outphasing Transmitter Using Class-E PAs and Asymmetric Combining: Part 2

By Ramon Beltran, RF Micro Devices; Frederick H. Raab, Green Mountain Radio Research; and Arturo Velazquez, CICESE Research Center

This article on Class-E PAs for Outphasing/Chireix modulation concludes with the detailed description of a 900 MHz prototype transmitter circuit

UHF Prototype

Class-E operation at UHF and microwave frequencies can be approximated by using transmission-line networks to control a finite number of harmonics [11, 12]. For

operation at UHF, the T-networks used in the 1.8 MHz prototype are replaced by transmission lines.

Second Harmonic Class-E PA Design

The selected active device for the transmission-line class-E2 PA is the SD57030 transistor provided by STMicroelectronics. It has a maximum drain voltage of 65 V. In an ideal class-E PA in the optimum operating mode with 50% duty cycle and a slope of zero [5], the peak drain voltage is $v_{Dmax} = 3.56 V_{DD}$. Since the peak varies with load impedance, a design for $v_{Dmax} = 4 V_{DD}$ or slightly more is prudent, which suggests $V_{DD} = 15$ V. For a 10-W output power the fundamental load resistance is [5]:

$$R_0 = 0.577 \frac{V_{DD}^2}{P_{out}} = 12.98 \Omega \quad (8)$$

The dc-input current is [5]:

$$I_{DC} = \frac{V_{DD}}{1.73 \cdot R_0} = 0.667 \text{ A} \quad (9)$$

where the peak drain current $i_{Dmax} = 2.84$ IDC corresponding to a satisfactory $i_{Dmax} = 1.89$ A, since the SD57030 is a 4-A peak current device.

The shunt capacitance required for optimum operation is given by:

$$C = \frac{0.1836}{2\pi f_0 R_0} = 2.5 \text{ pF at } 900 \text{ MHz} \quad (10)$$

Since the drain capacitance of the SD57030 is 36.5 pF at 900 MHz, true transient class-E operation is not possible.

The class-E configuration is therefore based upon a second-harmonic approximation to class-E operation. A second-harmonic approximation of class E (class E2) is achieved by creating at the drain a fundamental-frequency impedance with equal resistance and positive reactance and a corresponding negative second harmonic reactance. The presence of the second harmonics shapes the voltage and current waveforms to boost efficiency, and the 90° phase difference between second-harmonic voltage and current prevents the generation of power at the second harmonic.

The design is based upon the waveform coefficients given in [12] and [13]; $\gamma_V = \gamma_I = 1.414$ and $\delta_V = \delta_I = 2.912$. Both the drain-voltage and drain-current waveforms are composed of fundamental-frequency and second-harmonic components. Their shapes are ideally identical, but the phases are shifted so that the second harmonics differ in phase by 90° and therefore consume no power. This causes the fundamental-frequency components to differ in phase by 45°, therefore the impedance at “virtual drain” (VD) is [12]:

$$Z_1 = R_1 + jR_1 \quad (11)$$

and

$$\rho = \frac{|Z_1|}{R_1} = 1.414 \quad (12)$$

To maintain the same relative level of second harmonic to fundamental in the current waveform as in the voltage waveform the second harmonic impedance must be

$$X_2 = j1.414R_1 \quad (13)$$

For a peak drain voltage of 65 V, the supply voltage must be no more than $65/\delta_V = 22.32$ V, hence $V_{DD} = 21$ V is selected. Since SD57030 has an on resistance $R_{ON} = 0.43 \Omega$, the effective supply voltage is $V_{eff} = 0.956V_{DD} = 20$ V. The fundamental frequency component of the drain-voltage waveform is [12, 13]:

$$V_{1m} = \gamma_V \cdot V_{eff} = 28.8 \text{ V} \quad (14)$$

The output voltage is then related to the waveform factors and load power factor by [12]:

$$V_{om} = \frac{V_{m1}}{\rho} = 20 \text{ V} \quad (15)$$

Given that the SD57030 is a 4-A peak device, the analysis can be based upon $i_{Dmax} = 2$ A, ensuring safe operation mode for the transistor. The dc-input current is then related to the waveform factors by

$$I_{DC} = \frac{i_{Dmax}}{\delta_I} = 0.687 \text{ A} \quad (16)$$

and the fundamental-frequency component of the drain-current waveform is therefore [12, 13]:

$$I_{1m} = I_{om} = \gamma_V \cdot I_{DC} = 0.971 \text{ A} \quad (17)$$

Consequently $P_o = (V_{om}I_{om})/2 = 9.71$ W and $P_{in} = V_{DD}I_{DC} = 13.74$ W, hence, the efficiency is $\eta = 0.707$. The efficiency is the same as that of the maximum efficiency second-harmonic class-F PA.

Second Harmonic Impedance of Optimum class-E

Optimum operation of an ideal class-E PA [5] requires a series load reactance of $X = 1.15R_o$ and a drain shunt susceptance of $0.1836/R_o$. Combining these produces the fundamental-frequency drain-load impedance. Since true transient class-E is not possible, it requires a harmonic termination at “virtual drain” (VD). Using the second harmonic approximation requires a VD impedance from eq. (11). Using (14) and (17) the magnitude of the fundamental-frequency impedance is given by

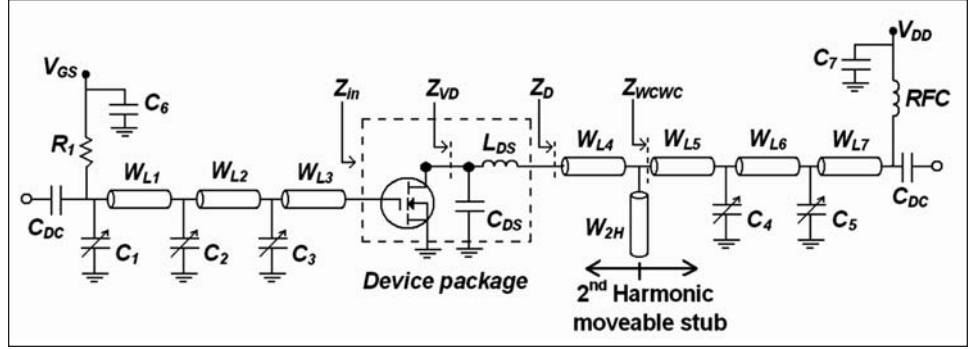


Figure 18 · Class-E2 PA schematic, $C_{DS} = 36.5$ pF and $L_{DS} = 0.45$ nH.

$$|Z_1| = \frac{V_{1m}}{I_{1m}} = 29.12 \Omega \quad (18)$$

and using eq. (12) yields; $R_1 = 20.6 \Omega$. From (11) and (13) the impedances to be presented at “virtual drain” (Z_{VD}) at fundamental-frequency and second harmonic must be respectively

$$Z_{VD} = Z_1 = 20.6 + j20.6 \Omega \quad (19)$$

$$X_2 = -j29.12 \Omega \quad (20)$$

At 900 MHz this corresponds to 6.07 pF.

Second Harmonic Stub and Matching Networks

The short at the n th harmonic can be provided by a quarter wavelength open stub. After determining the drain-terminal impedance (Z_{VD}) required to producing the desired reactance X_n at the highest harmonic used, the position of the highest-order harmonic stub must be determined. It can be approximately calculated by

$$\alpha = \arctan\left(\frac{X_n}{R_L}\right) \quad (21)$$

Above, α represents the distance at which the open stub with impedance R_L , must be placed from V_D . A second harmonic stub of $R_L = 25 \Omega$ must be placed at approximately $\alpha = 25^\circ$ of electrical length from V_D , in order to produce the required second harmonic impedance from eq. (20). Transmission line W_{L4} in Figure 18 is used to serve the purpose.

After determining the distance of the second harmonic stub from “virtual drain” the fundamental frequency impedance matching can be performed by a line-capacitor-line-capacitor (WCWC) section, to provide the required impedance Z_{VD} at “virtual drain.” It is imperative that the parasitic drain capacitance and inductance

	Pin (dBm)	Pout (Watts)	Drain efficiency
PA1	30	10	71.0 %
PA2	30.1	10	71.0 %

Table 1 · Measured class-E2 PA characteristics.

must be taken into account for proper impedance termination at virtual drain, the SD57030 model were provided by STMicroelectronics and has a drain capacitance of 36.5 pF and inductance of 0.45 nH. Because the stub creates a short on the main transmission line, the portion of the output network to the right of the stub has no effect upon that harmonic impedance.

The input matching network is designed using the measured reflection coefficient S_{11} parameter and properly converted to the equivalent impedance Z_{in} , when the transistor drain is open and short circuited with gate bias at threshold voltage $V_{GS} = 2.6$ V. The input impedance for both states is the same as that provided by the transistor model. Both input and output matching networks are composed of variable capacitors suitable to work at UHF frequencies in order to have tuning options and/or slight alignment for the desired PA performance.

Amplifiers' Performance

Two identical class-E2 amplifiers were built in order to implement the outphasing system. It is important to align both amplifiers to behave the most identical possible. Each PA is driven by a linear amplifier (class-AB); with a power of 30 dBm, these in turn are driven by a signal generator with -5 dBm output power. The PAs' performance is shown in Table 1. Both PAs behave very much like each other. They were built on separate PCBs using the GML1000 substrate, with a dielectric constant $\epsilon_r = 3.2$ for a substrate thickness of 30 mil.

The amplifiers are first tuned as

class B without the second harmonic stub. This is carried out by adjusting the trimmers to obtain the required output power and best efficiency. The tuning procedure first adjusts the input network for best VSWR using a network analyzer with the transistor biased at the design voltage ($V_{DS} = 20$ V and $V_{GS} = 2.6$ V) and the output port terminated in 50Ω loaded to prevent undesired signal reflections.

Then the output network trimmers are adjusted for best output power and efficiency.

Once the amplifiers are tuned as class B, the moveable second-harmonic stub is placed on the main transmission line (Fig. 19) close to the transistor drain at an approximated distance computed in eq. (21). Its position is adjusted to achieve the best efficiency and desired output

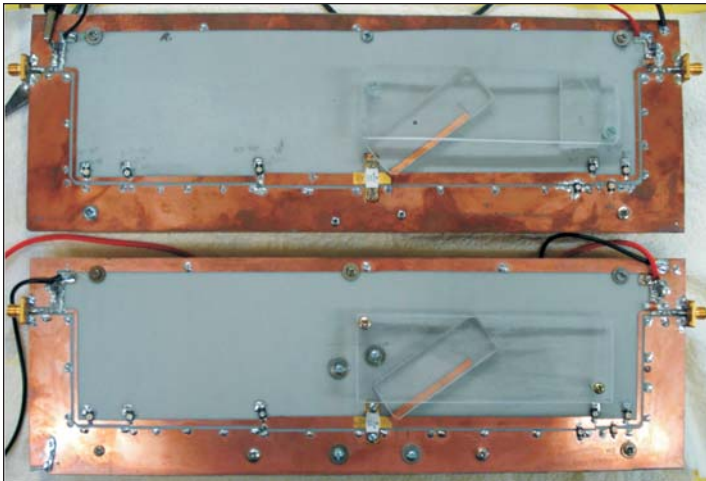


Figure 19 · Class-E amplifiers with moveable stubs.

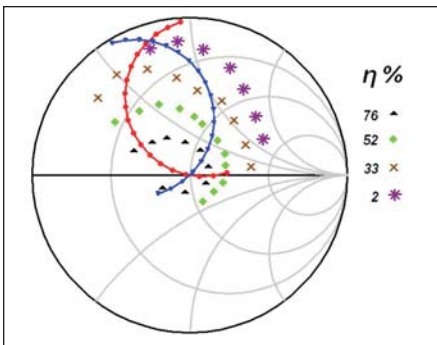


Figure 20 · Class-E PA efficiency contours and optimum impedance loci for PA1 (circular markers) and PA2 (triangular markers).

power. Since the trimmers must be readjusted as the stub is moved, this process is fairly tedious. The final distance of the second harmonic moveable stub from the transistor drain can be closer than the computed one by eq. (21) due to variation in fabrication process, substrate characteristics, and transistor parasitic. The measured performance of Table 1 shows that drain efficiency is slightly better than the predicted value.

Load-pull Characterization

At HF the true transient class-E is possible. The load-pull contours for the ideal class-E PA are shown in previous section, then it shows the required transmission line length to present the PAs with the optimum

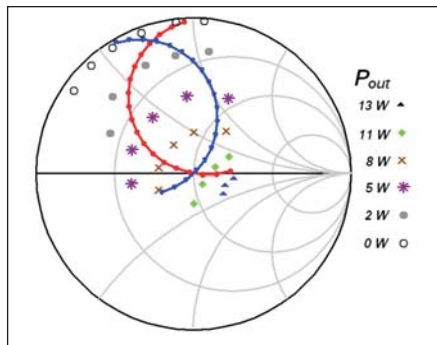


Figure 21 · Class-E PA P_{out} contours and optimum impedance loci for PA1 (circular markers) and PA2 (triangular markers).

impedance loci for proper operation in outphasing. At UHF, class-E operation is approximated with transmission-line networks. Since this is a different output circuit, it is necessary to characterize these PAs experimentally to determine the desired impedance loci. The experimentally determined load-pull contours are shown in Figures 20 and 21. Both amplifiers present similar regions for efficiency and output power as they were carefully tuned to have identical amplifiers.

Design of Asymmetric Combiner

Line stretchers (Fig. 22) are used for initial development and testing of the asymmetric combiner. The line stretchers are very useful since they

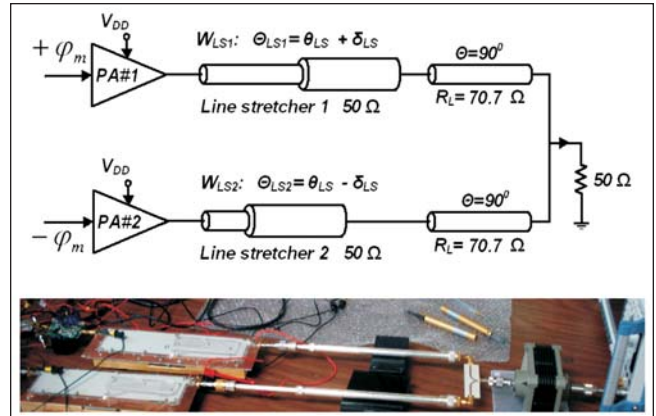


Figure 22 · Class-E PAs asymmetric combining using stretchers.

can be shortened or expanded to present the PAs with the required impedances; hence, they work around the best efficiency points in Fig. 20.

The required optimum impedance loci seen by the PA1 (circular markers) and PA2 (triangular markers) is shown in Fig. 21. This is verified for different set ups of the line stretchers around the best achievable efficiency along all amplitude outputs. The system best efficiency requires the line stretchers to have $\theta_{LS} = 126.5^\circ$ and $\delta_{LS} = 13.5^\circ$, hence $W_{LS1} = 140^\circ$ and $W_{LS2} = 113^\circ$ (solid line in Fig. 23).

The effects on efficiency for other values of θ_{LS} and δ_{LS} than the optimums are also shown in Fig. 23. θ_{LS} is varied +/- 10 with δ_{LS} fixed at the optimum value, so that $\theta_{LS} = 136.5^\circ$ and $\delta_{LS} = 13.5^\circ$, hence $W_{LS1} = 150^\circ$ and $W_{LS2} = 123^\circ$ (inverted triangle markers in Fig. 23), and $\theta_{LS} = 116.5^\circ$ and $\delta_{LS} = 13.5^\circ$, hence $W_{LS1} = 130^\circ$ and $W_{LS2} = 103^\circ$ (circular markers in Fig. 23).

Then δ_{LS} is varied to $+5^\circ$ and $+10^\circ$ while θ_{LS} remains at the optimum, so that $\theta_{LS} = 126.5^\circ$ and $\delta_{LS} = 18.5^\circ$, hence $W_{LS1} = 145^\circ$ and $W_{LS2} = 108^\circ$ (asterisk markers in Fig. 23) and $\theta_{LS} = 126.5^\circ$ and $\delta_{LS} = 23.5^\circ$, hence $W_{LS1} = 150^\circ$ and $W_{LS2} = 103^\circ$ (point markers in Fig. 23). Finally, θ_{LS} is set at -10° less from the optimum and δ_{LS} is set at $+5^\circ$ from its optimum value, so that $\theta_{LS} = 116.5^\circ$ and $\delta_{LS} = 18.5^\circ$ (dia-

OUTPHASING TRANSMITTER

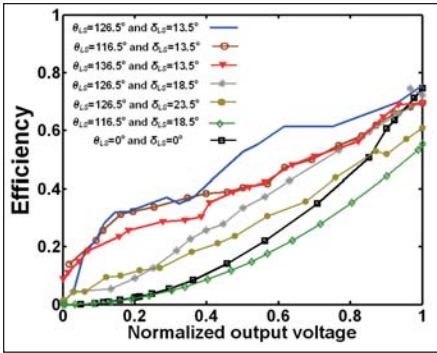


Figure 23 · Efficiency vs. output voltage for various line stretchers settings.

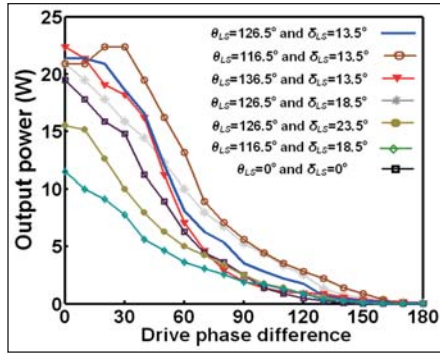


Figure 24 · Output power vs. drive phase difference for various line stretchers settings.

mond markers in Fig. 23).

Efficiency for $\theta_{LS} = 0^\circ$ and $\delta_{LS} = 0^\circ$ (quarter wave length lines combiner only) is also presented in Fig. 23 (square markers), it can be compared to the efficiency of an outphasing using hybrid combiner, where the advantageous of using asymmetric combiner is evidenced.

Implementation of Asymmetric Combiner

After the final adjustment of the asymmetric combiner using line stretchers the two class-E2 PAs are

built on the same board. The asymmetric outphasing system schematic is shown in Figure 25. Both amplifiers input and output networks are then reduced in length. This actually moves their impedance loci by certain amount but the same technique using line stretcher can be applied in order to re-adjust the asymmetric combiner for best output and efficiency. Once the line stretchers lengths are determined, the two class-E2 PAs are built on the same board as well as the asymmetric combiner using phase transmission lines (Fig. 26). The

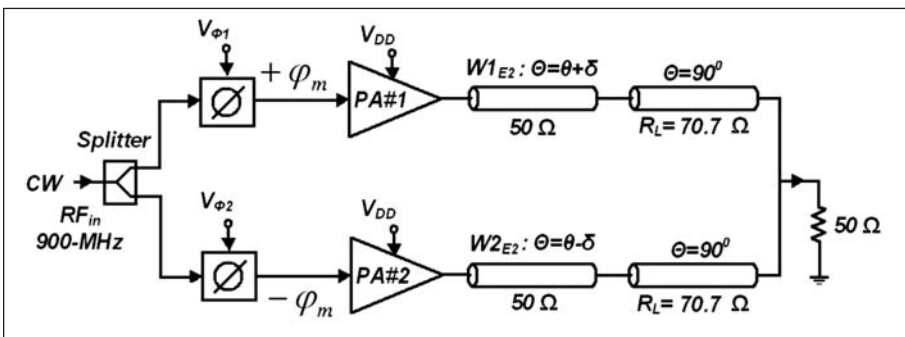


Figure 25 · UHF Asymmetric class-E2 transmitter.

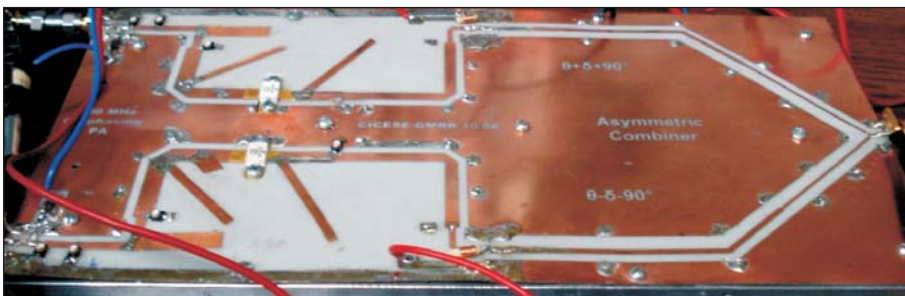


Figure 26 · Class-E2 PAs and asymmetric combiner prototype layout.

input network is tuned using the input trimmers and opened stubs located in judicious locations on the input network to improve input match (or VSWR), the moveable second harmonic stubs remain practically at the same distance from the device drain.

Phase variation is performed by two voltage controlled phase shifters from Mini-Circuits (JSPHS-1000). A control voltage from 0 to 12 V varies the drive phase difference $\Delta\phi_m$ from 0 to 180°, Fig. 25.

The final asymmetric system efficiency characteristics are shown in Figure 27. The efficiency is improved by a factor of 1.375 or more from zero to 0.6 normalized output voltage compared with that of ideal class-B PA. This in turns increases average efficiency considerably by a good percent for signals with large peak-to-envelope power ratios. It is also compared with a measured class-B PA (amplifier with no harmonic stub) with efficiency improvements for almost all output amplitudes.

The output power characteristic is shown in Figure 28. The peak output power (PEP- $\Delta\phi_m 0^\circ$) is a combination of output power from PA1 and PA2 of 21.34 W. They maintain the same output amplitude for drive phases $\Delta\phi_m$ from 0 to 20°. Then the system output power decreases to zero in a non-linear curve of output amplitude over the drive phase difference. Even though the system presents a very good dynamic range it is evident that the asymmetric system requires to be linearized.

Amplifier Linearization Using Predistortion

The linearization of the asymmetric system started with AM-AM and AM-PM characterization. The test setup is shown in Figure 29. The input of the asymmetric system is connected to the input port of the network analyzer, a divider splits the CW input signal of 900 MHz into two equal amplitude and phase signals to

OUTPHASING TRANSMITTER

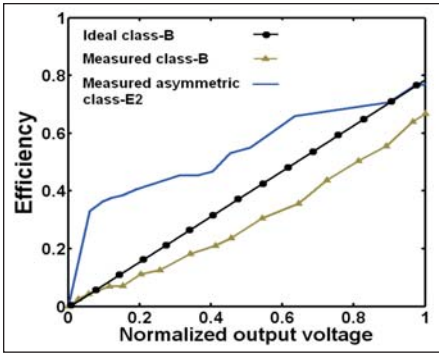


Figure 27 . Asymmetric class-E2 outphasing efficiency vs. output voltage.

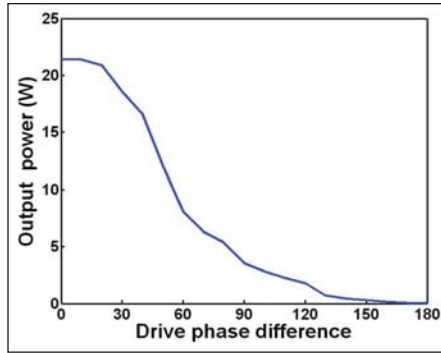


Figure 28 . Output power characteristic vs. phase difference between driving signals.

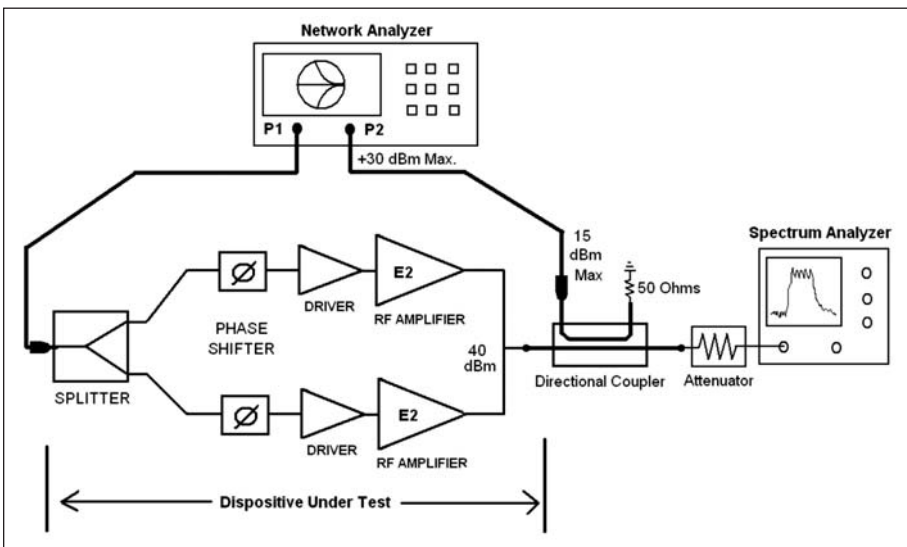


Figure 29 . AM-PM characterization test bench.

feed the voltage controlled phase shifters. The constant amplitude but phase varied signals are sent to the linear drivers to provide the required saturation input power to achieve

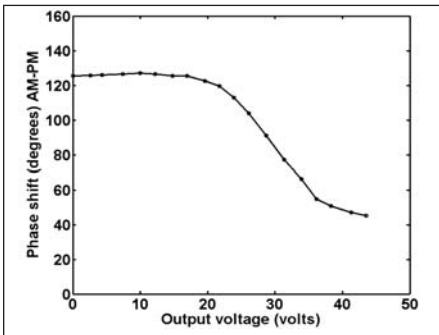


Figure 30 . AM-PM characteristics in terms of output voltage amplitude.

class-E2 operation. The asymmetric combined outputs are then sent to a well characterized directional coupler with a coupling factor of 25 dB. The coupled port is connected to the port

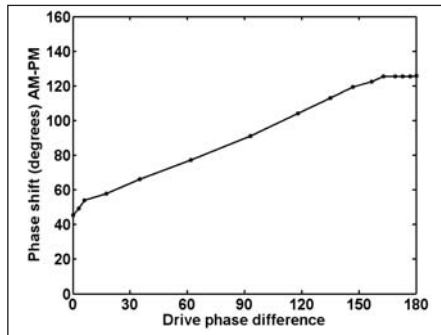


Figure 31 . AM-PM characteristics in terms of drive signals phase difference.

2 of the network analyzer attenuating the PAs system output by 25 dB, hence, the analyzer receives no more than 15 dBm with a phase shift of 30° from the system output. The directional coupler attenuation in forward direction is just 0.095 dB and 39.79 dB of return loss. The output of the directional coupler is then connected to a 32.5-dB (at 900-MHz) attenuator before the spectrum analyzer. Port 1 is fixed at 900 MHz and delivers a power up to 5 dBm, since the linear drivers has a gain of 35 dB, -5 dBm from port 1 is enough to boost input power to saturate the class-E2 PAs that requires 30 dBm of drive. The AM-PM conversion is measured with the VNA through the port 2 and proper correction is applied to get the phase shift at the asymmetric outphasing output. Besides, it is possible to observe the spectra in the spectrum analyzer and get the AM-AM characteristics.

Since the input power is a constant amplitude (but phase modulated) signal and the output amplitude varies according to the input signals phase difference, the AM-AM and AM-PM characteristics are measured in terms of drive phase difference instead of a varying input power as in a conventional amplifier. The output power varies as phase difference increases; hence, it is necessary to vary drive phases by varying control voltages of the phase shifters from zero ($\Delta\phi_m = 0^\circ$ -PEP) to 12 volts ($\Delta\phi_m = 180^\circ$ -zero output) in order to

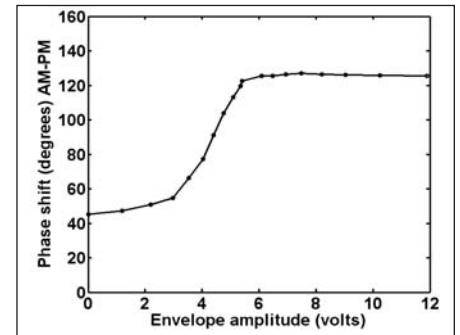


Figure 32 . AM-PM characteristics in terms of envelope amplitude (phase shifter control voltage).

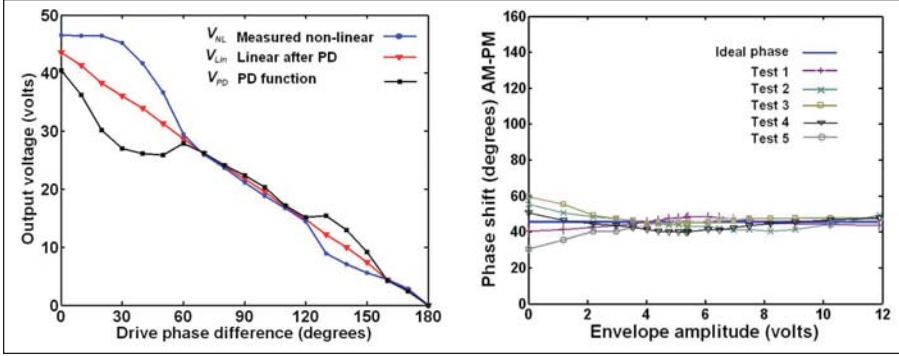


Figure 33 - Output voltage vs. drive phase difference (left), and corrected system phase shift for four tests (right).

measure the system AM-PM conversion. It can be shown in terms of output voltage as in Figure 30, or in terms of drive phase difference, Figure 31, or even in terms of envelope amplitude (phase shifter control voltage), Figure 32. Any of the three AM-PM conversion measurements can be used to apply predistortion in order to correct the system phase shift. For convenience system phase shift (AM-PM) vs. output voltage is used, this measured also avoid confusion between drive phase difference $\Delta\phi_m$ and system phase shift (AM-PM). In Fig. 30, an AM-PM conversion from 125.5° to 45.5° is observed. This needs to be corrected for linear operation.

The output amplitude or gain conversion is also taken in terms of drive phase difference $\Delta\phi_m$ as shown in Figure 28; the AM-AM conversion can be corrected in term of amplitude output power or voltage as shown in Figure 33.

Amplitude predistortion is first applied to obtain a linear response of the system amplitude output. A predistortion (PD) function is devised as the inverse of the system non-linear output voltage response by

$$V_{PD} = V_{NL} + 2 \cdot (V_{Lin} - V_{NL}) \quad (22)$$

where V_{NL} is the non-linear system amplitude output, V_{Lin} is the obtained linear response of output amplitude and V_{PD} is the inverse of

the non-linear system amplitude, The PD function can be used to predistort a given envelope signal as shown in Figure 33.

Phase predistortion is accomplished by using a look-up table with amplitude predistortion on. The AM-PM conversion is corrected to achieve an rms error of 2.5° with predistorted data stored in a LUT that predistorts a specified envelope signal as

described below. After a warm-up time of half an hour the first measured is taken, and then four different measures were taken at 1 hour time span.

Once the amplitude and phase are corrected the linearity characteristics of the asymmetric class-E2 outphasing are tested using the standard linearity measures such as the two-tone and ten-tone envelope signals. The amplitude modulation signals are introduced through the voltage controlled phase shifters (Fig. 34). The envelope signals were produced by software using MATLAB[®] and then they are converted to sound files in order to be able to send them through the PC sound card, it can be accomplish by using the *sound(.)* function or conversion of a the data vector (voltages from 0 to 12 volts) to .wav files using the *wavwrite(.)* function, Figure 35. The utilized PC sound card maximum output voltage is ± 1 volt, it is necessary therefore to adequately

OUTPHASING TRANSMITTER

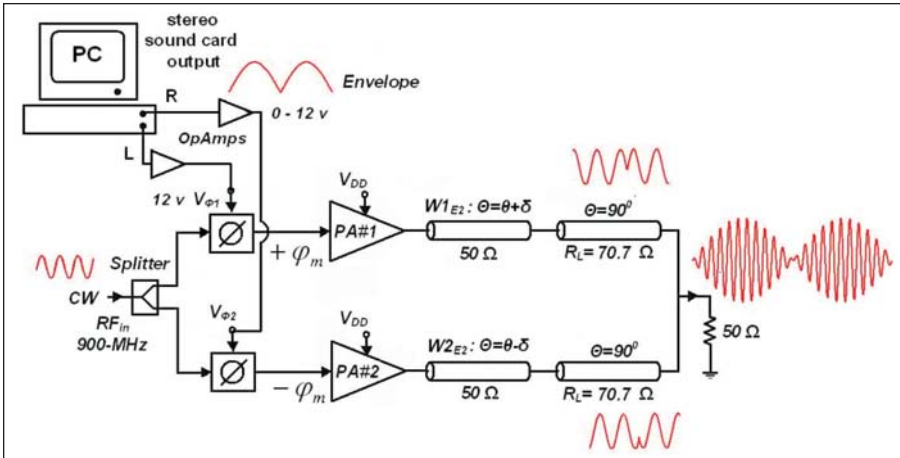


Figure 34 · Outphasing modulation using voltage controlled phase shifters.

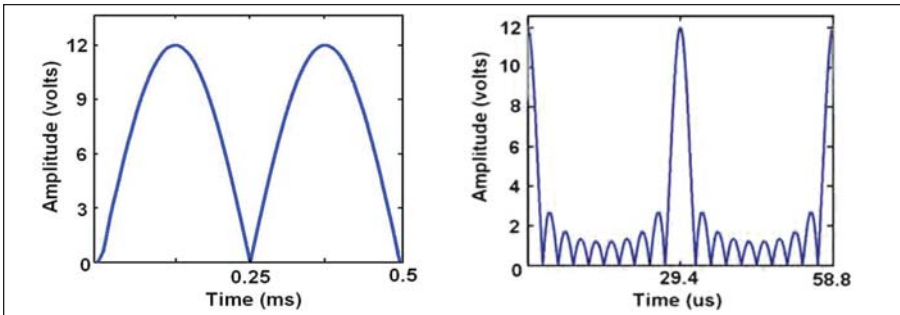


Figure 35 · Two-tone and ten-tone signals produced by software.

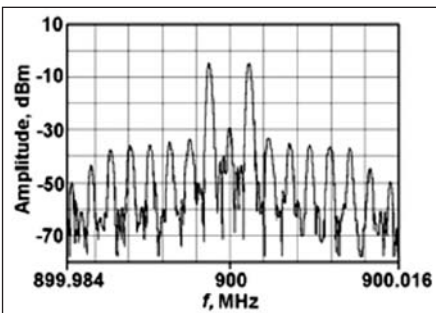


Figure 36 · Spectrum of the 2-tone envelope signal.

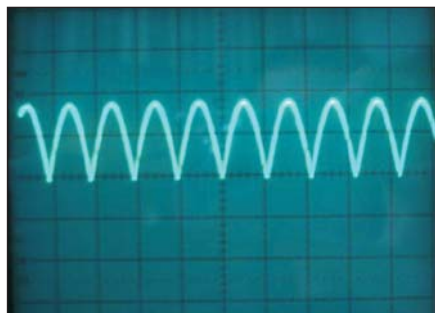


Figure 37 · Detected two-tone envelope (horizontal 0.5 ms/div, vertical 5 V/div).

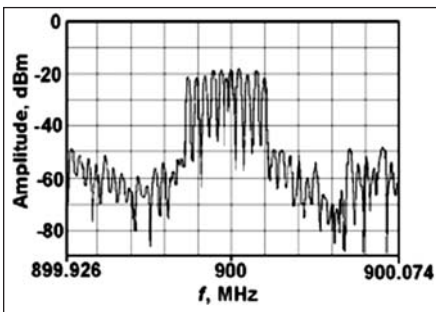


Figure 38 · Spectrum of the 2-tone and 10-tone signal.

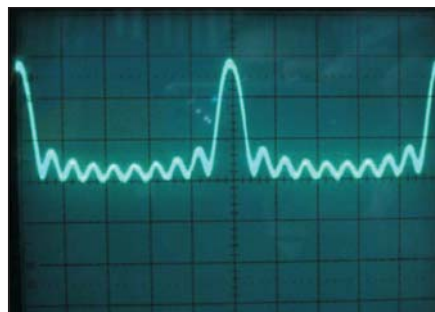


Figure 39 · Detected ten-tone envelope (horizontal 6 us/div, vertical 5 V/div).

interface with the phase shifter. This is accomplished by a couple of operational amplifiers that amplify the sound card signal to set them from zero to 12 volts, Figure 34.

Since the phase shifters have a 50 kHz control bandwidth, a two-tone and ten tone envelope of 2 and 17 kHz respectively can be easily sent to the control voltage pin of the phase shifter, this means that the phase shifters will produce the system peak output power when the envelope signal will be at its peak of 12 volts and this is therefore 180° of phase shift, since both phase shifters are set at 12 volts initially (180° phase shifter), the output from each PA are added in-phase producing the system PEP ($\Delta\phi_m = 0$). When the envelope signal is at its minimum value, this means zero control voltage of the phase shifters and hence 0° phase shift, since one of the phase shifter is set at 12 volts (180°), the PAs outputs are added out-phase producing zero output voltage ($\Delta\phi_m = 180^\circ$). Then outphasing modulation is achieved.

The envelope waveforms are pre-distorted according to the amplitude and phase corrections described above. The measured two tone spectra is shown in Fig. 36, the envelope signal frequency (modulation frequency) is 2 kHz as mentioned before. The detected envelope is shown in Figure 37 and. The third order IM products are at 28.98 dBc.

The spectrum of a ten-tone signal with modulation frequency of 17 kHz is shown in Figure 38. This is an “all-cosine” signal with a 10-dB peak-to-average ratio, which is typical of a modern OFDM signal. The detected envelope is shown in Figure 39. The third order IM products are at 32 dBc.

Conclusions

Maintaining good instantaneous efficiency over a wide range of amplitudes will result in significant improvements in the average efficiency when producing amplitude-modulated signals. Potential applica-

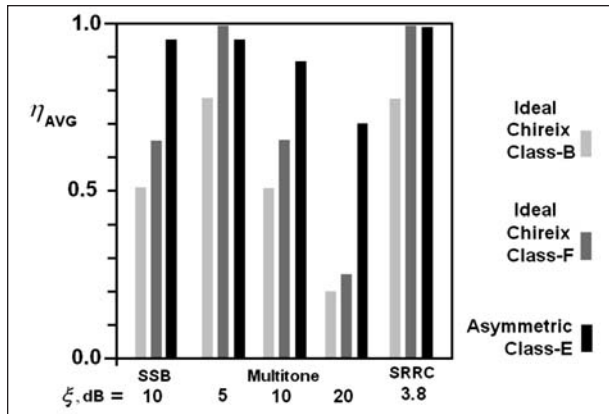


Figure 40. Predicted average efficiency for various signals for an ideal system.

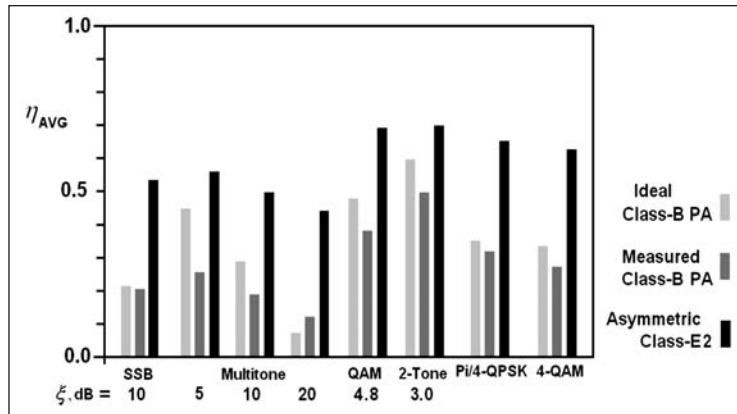


Figure 41. Predicted average efficiency for various signals for the UHF system.

tions include power amplifiers for W-CDMA, WiMAX, and other modern wide-band communication systems.

The predicted average efficiency of an ideal asymmetric class-E outphasing is 98.7% for a signal with a square-root raised-cosign (SRRC; $\pi/4$ -QPSK) envelope (3.8-dB peak to average ratio) and 88.7% for a Rayleigh-signal with a 10-dB peak to average ratio (ξ). In contrast, the average efficiencies for an ideal linear class-B PA are only 51.8% and 28%, respectively. Figure 40 shows average efficiencies comparison among optimized ideal Chireix-outphasing with class-B and F PAs and the asymmetric class-E outphasing for SSB ($\xi = 10$ dB). Multitone (Rayleigh envelope with $\xi = 5$, $\xi = 10$ and $\xi = 20$ dB) and SRRC ($\xi = 3.8$ dB). The highly reactive loads make a Chireix transmitter with class B and F PAs very inefficient at low outputs, this impact on the average efficiencies, Figure 40.

The average efficiencies for the UHF prototype are shown in Figure 41. It is appear that the average efficiencies are considerably greater than those for the ideal class-B PA, i.e. for a 10 tone signal that is typical in OFDM systems, the average efficiency for the 900 MHz asymmetric class-E2 outphasing is 49.78% in contrast with 28% for the ideal class-B PA. For a $\pi/4$ -QPSK signal the average efficiency is 66% when an ideal

class-B PA achieves just 35.35%. Other efficiencies are compared in Fig. 41.

The ideal asymmetric class-E outphasing offers significant improvement in average efficiency for amplitude modulated signals. The asymmetric combining technique can be applied not only for ideal class-E PA but also for any amplifier class that attempt to operate in outphasing, in this case it is necessary to know the efficiency and output power impedance loci in order to present them to the two PAs for best outphasing output (dynamic range) and efficiency.

References

Part 1 of this article, including References 1-9 was published in the April 2011 issue of High Frequency Electronics, and is available in the Archives section of our web site.

10. R. Beltran, F. H. Raab, and Arturo Velazquez, "HF outphasing transmitter using class-E power amplifiers," *MTT-S International Microwave Symposium Digest*, 2004, Boston, MA, Jun. 7-12, 2009.

11. T. B. Mader, Z. B. Popovic, "Transmission line high efficiency class-E amplifier," *IEEE Microwave and Guided Wave Letters*, Vol. 5, no. 9, September, 1995.

12. F. H. Raab, "Class-E, Class-C, and Class-F Power amplifiers based

upon a finite number of harmonics," *IEEE Transactions on Microwave Theory and Techniques*, vol. 49, no. 8, August 2001.

13. F. H. Raab, "Maximum efficiency and output of class-F power amplifiers," *IEEE Trans. Microwave Theory and Techniques*, vol. 47, pp. 1162-1166, June, 2001.

Author Information

Ramon Beltran received his M.Sc and PhD degrees in high-frequency electronics from CICESE Research Center in 2004 and 2009, respectively. He is a Sr. Design Engineer with RF Micro Devices involved in power amplifier design for cellular handsets in the Advanced Development Group. His research interests are focused on high-efficiency power amplifiers and transmitters. He can be contacted at ramon.beltran@rfmd.com

Frederick H. Raab is Chief Engineer and Owner of Green Mountain Radio Research, a consulting firm which he founded in 1980. He received B.S., M.S., and Ph.D. degrees in electrical engineering from Iowa State University in 1968, 1970, and 1972. Professional achievements include publication of over 100 technical papers and award of twelve patents. He is an IEEE Fellow and member of HKN, AOC, AFCEA, RCA (fellow), and ARRL. "Fritz" can be reached by e-mail at: f.raab@ieee.org